Temperature and density dependence of the nucleon mean free path in the relativistic mean field model

Han Yinlu
China Institute of Atomic Energy, P.O. Box 275(41), Beijing 102413, People's Republic of China

Zhang Zhengjun and Sun Xiuquan
Department of Physics, Northwest University, Shaanxi, 710069, People's Republic of China
(Received 31 December 1996)

The nucleon mean free path is obtained based on the relativistic σ-ω model, the thermofield dynamics and the relativistic Dirac-Brueckner-Hartree-Fock results which includes the important medium effects at finite temperature in nuclear matter. The temperature and density dependence of the nucleon self-energy in nuclear matter is derived from the effective Lagrangian taking diagrams up to fourth order into account. The calculated results of the nucleon mean free path at zero temperature are in good agreement with the experimental data in normal nuclear matter. [S0556-2813(97)01206-5]

PACS number(s): 21.65.+f, 24.10.Jv, 24.10.Ht, 24.10.Cn

I. INTRODUCTION

One of the most fundamental properties characterizing the propagation of a nucleon in the nuclear medium is its mean free path. The nucleon mean free path is one of the useful concepts in nuclear physics for summarizing a large number of experimental data in nuclear reaction. Furthermore, in the investigation of heavy-ion reactions, it is of great relevance to know the mean free path of a nucleon when the immediate medium is the overlap of the projectile and the target, especially, the temperature and density dependence of the nucleon mean free path is of great importance.

The calculation of the nucleon mean free path has been done in the framework of nonrelativistic dynamics [1–9], based on, e.g., the phenomenological Skyrme interaction. A characteristic of the early theoretical studies [1,2] is the underestimation of the nucleon mean free path as compared to the empirical values. The proper treatment of the nonlocality of the nucleon optical potential resolves much of the discrepancy between the theoretical prediction and empirical data [3,5]. The nonlocality of the nucleon optical potential leads to the reduction of the nucleon mass, as Negele and Yazaki pointed out [3], the reduction of the effective mass plays an important role in enhancing the theoretical mean free path.

The relativistic calculations of the nucleon mean free path have been done [10–18] based on the relativistic model. Because relativistic models always produce effective masses which are significantly smaller than 1 [19], it would be of interest to see the relativistic effect on the mean free path of the nucleon. Because the experimental data [20,21] of the nucleon mean free path come from the analysis of the experimental data of the neutron and proton reaction cross section and scattering cross section, it is important to perform a microscopic calculation of the nucleon mean free path from the optical model potential theoretically. The Schrödinger equivalent potential of the relativistic microscopic optical potential has been derived [22,23] in nuclear matter at zero temperature based on the relativistic σ-ω model of Walecka [24], and has been used to systematically analyze intermediate and high-energy nucleon-nuclei reaction cross sections, the differential cross section, analyzing power, and spin rotation function at zero temperature for $E \leqslant 1000$ MeV [25,26]. The calculated results show that the Schrödinger equivalent potential of the relativistic microscopic optical potential based on the relativistic σ-ω model of Walecka could reproduce the experimental data for various target nuclei satisfactorily.

Encouraged and motivated by the success of the relativistic microscopic optical potential calculation of a nucleon based on the relativistic σ-ω model of Walecka, we study the temperature and density dependence of the nucleon mean free path based on the relativistic σ-ω model of Walecka, the relativistic Dirac-Brueckner-Hartree-Fock approach [27,28] which includes the important medium effects, and the thermofield dynamics [29,30] in this paper. The temperature and density dependence of the nucleon self-energy (relativistic microscopic optical potential) is derived. This work is a continuation of our previous works [10,13,18].

The formulation of the temperature and density dependence of the nucleon self-energy and mean free path are presented in Sec. II. The results and discussion are given in Sec. III. Finally, in Sec. IV, we give a brief summary and conclusion.

II. TEMPERATURE AND DENSITY DEPENDENCE OF THE NUCLEON SELF-ENERGY AND MEAN FREE PATH IN NUCLEAR MATTER

The relativistic σ-ω model of Walecka contains neutral scalar σ mesons, neutral vector ω mesons, and nucleons. This model is responsible for the observed short-range repulsive and long-range attractive force between two nucleons in the static limit. We extend Walecka's model to the cases of finite temperature and various nuclear densities based on thermofield dynamics and the relativistic Dirac-Brueckner-Hartree-Fock approach. The effective Lagrangian is given as

$$\pounds=\sum_a \varepsilon_a P_a\Big[\overline{\psi^{(a)}}(i\gamma^\mu\partial_\mu-m)\psi^{(a)}+\frac{1}{2}(\partial^\mu\phi^{(a)}\partial_\mu\phi^{(a)}-m_\sigma^2\phi^{(a)2})-\frac{1}{4}F^{(a)}_{\mu\nu}F^{(a)\mu\nu}+\frac{1}{2}m_\omega^2V_\mu^{(a)2}-g_\sigma(\rho)\overline{\psi^{(a)}}\phi^{(a)}\psi^{(a)}-g_\omega(\rho)\overline{\psi^{(a)}}\gamma^\mu V_\mu^{(a)}\psi^{(a)}\Big], \quad (1)$$

where $\psi^{(a)}$, $\phi^{(a)}$, and $V^{(a)}$ are the nucleon, σ-, and ω-meson field operators, respectively, and the explicit expressions of the field operators were obtained from Ref. [31]. The index $a(=1,2)$ specifies a component of the thermal doublet. The first component $(a=1)$ is physical, and the other one $(a=2)$ is fictitious. The values of the nucleon and ω-meson masses are taken from the experiment, $m=939$ MeV and $m_\omega=783$ MeV, while the mass of the hypothetical σ meson is fixed at $m_\sigma=550$ MeV, which is commonly used in the NN interaction. P_σ is the ordering operator and the sign factor ε_a is 1 or -1 when the a is 1 or 2, respectively. $g_\sigma(\rho)$ and $g_\omega(\rho)$ are the density-dependent coupling constants.

The Dyson equation for the temperature and density-dependent Dirac field is

$$G^{(ab)}(k_\mu,\beta,\rho)=G^{0(ab)}(k_\mu,\beta,\rho)+\sum_{cd} G^{0(ac)}(k_\mu,\beta,\rho)\times\Sigma^{(cd)}(k_\mu,\beta,\rho)G^{(db)}(k_\mu,\beta,\rho), \quad (2)$$

where $\Sigma^{(cd)}(k_\mu,\beta,\rho)$ is the temperature and density dependence of the proper nucleon self-energy, $\beta(=1/\mathrm{KT})$ is nuclear temperature, and ρ is the nuclear matter density. We have omitted the spinor index for simplicity. Because of physical considerations the $\Sigma^{(11)}$ is the only quantity that needs to be calculated. The temperature and density dependence of the nucleon self-energy obtained by the meson exchanges can, in general, be written as

$$\Sigma(k_\mu,\beta,\rho)=\Sigma^{(11)}(k_\mu,\beta,\rho)=\Sigma_S(k_\mu,\beta,\rho)+\gamma^0\Sigma_0(k_\mu,\beta,\rho)+\vec{\gamma}\cdot\vec{k}\Sigma_V(k_\mu,\beta,\rho), \quad (3)$$

where Σ_S, Σ_0, and Σ_V denote the scalar, vector, and three-vector components of the nucleon self-energy, respectively. In general, they are a function of the four-momentum k_μ of a nucleon, the nuclear temperature, and density.

The temperature and density dependence of the real part of the nucleon self-energy contains Hartree contributions [Fig. 1(a)] as well as Fock contributions [Fig. 1(b)] based on Walecka's model and thermofield dynamics. The explicit expressions of them is [12,17,32]

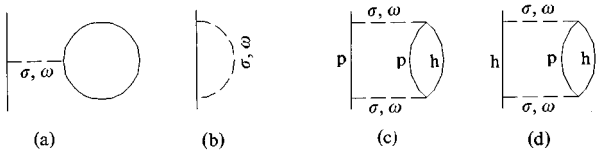

FIG. 1. Feynman diagrams for the calculation of the nucleon self-energy in nuclear matter. (a) Hartree diagrams, (b) Fock diagrams, (c) the fourth-order diagrams (polarization), (d) the fourth-order diagrams (correlation). The dashed lines denote the meson propagator. The solid lines represent the relativistic Hartree-Fock nucleon propagators.

$$\Sigma_S(k_\mu,\beta,\rho)=-\frac{\lambda g_\sigma^2(\rho)}{\pi^2m_\sigma^2}\int_0^\infty q^2dq\frac{m^*}{E_q^*}\sin^2\theta_{E_q}+\frac{1}{16\pi^2k}\int_0^\infty qdq\frac{m^*}{E_q^*}[g_\sigma^2(\rho)\Theta_\sigma(k,q)-4g_\omega^2(\rho)\Theta_\omega(k,q)]\sin^2\theta_{E_q}, \quad (4)$$

$$\Sigma_0(k_\mu,\beta,\rho)=\frac{\lambda g_\omega^2(\rho)}{\pi^2m_\omega^2}\int_0^\infty q^2dq\sin^2\theta_{E_q}+\frac{1}{16\pi^2k}\int_0^\infty qdq[g_\sigma^2(\rho)\Theta_\sigma(k,q)+2g_\omega^2(\rho)\Theta_\omega(k,q)]\sin^2\theta_{E_q}, \quad (5)$$

$$\Sigma_V(k_\mu,\beta,\rho)=-\frac{1}{8\pi^2k^2}\int_0^\infty qdq\frac{q^*}{E_q^*}[g_\sigma^2(\rho)\Phi_\sigma(k,q)+2g_\omega^2(\rho)\Phi_\omega(k,q)]\sin^2\theta_{E_q}, \quad (6)$$

where

$$m_k^*=m+\Sigma_S(k_\mu,\beta,\rho),\quad \vec{k}^*=\vec{k}[1+\Sigma_V(k_\mu,\beta,\rho)],$$

$$k_0^*=k_0-\Sigma_0(k_\mu,\beta,\rho)=\sqrt{k^2+m^{*2}},$$

$$\Theta_i(k,q)=\ln\left|\frac{A_i(k,q)+2kq}{A_i(k,q)-2kq}\right|,$$

$$\Phi_i(k,q)=\frac{A_i(k,q)\Theta_i(k,q)}{4kq}-1,$$

$$A_i(k,q)=k^2+q^2+m_i^2-(k_0-E_q)^2,\quad \lambda=2,\quad i=\sigma,\omega. \quad (7)$$

The first terms of the Σ_S and Σ_0 in Eqs. (4) and (5) are just the Hartree terms, which are energy independent. The remaining terms are Fock terms, which are almost $1/k$ energy dependent. Σ_V is a very small negative three-vector component which is purely contributed from the Fock term. The coupled nonlinear integral equations (4)–(7) should be solved self-consistently.

The lowest order contribution to the temperature and density dependence of the imaginary part of the nucleon self-energy is the fourth-order diagram from the meson exchange

point of view. The diagrams are characterized with $2p1h$ [Fig. 1(c)] and $2h1p$ [Fig. 1(d)] intermediate states. The nucleon lines in the diagrams are described by dressed nucleon propagators, which correspond to performing the calculation on the Hartree-Fock ground state and taking into account all Hartree-Fock insertions. Since the Hartree-Fock self-energy of a nucleon is weakly momentum dependent, in the calculation of the imaginary part we make a simple assumption: the dressed nucleon propagator entering in the calculation is constructed by the real nucleon self-energy at the Fermi momentum and by neglecting the small, real three-vector self-energy of the nucleon. The explicit expressions for the temperature-dependent imaginary part of the nucleon self-energy have been given in Refs. [13,18]. The derivation of the temperature-dependent imaginary part of the nucleon self-energy from Walecka's model and thermofield dynamics has been discussed in Refs. [13,18]. For this work, the detailed expressions for the temperature and density dependence of the imaginary part (scalar component W_S, vector component W_0, and three-vector component W_V) of the nucleon self-energy terms are similar to the expressions of temperature-dependent imaginary part of the nucleon self-energy terms in Ref. [13], but with the coupling constants for the σ-meson and ω-meson exchange replaced by the density-dependent ones as determined in the nuclear matter relativistic Dirac-Brueckner-Hartree-Fock calculation.

The detailed studies of the relativistic Dirac-Brueckner-Hartree-Fock and relativistic-density-dependent Hartree theory on properties of nuclear matter as well as finite nuclei by Machleidt [27], Brockmann and Toki [33] clearly show that the scalar and vector coupling constants should be density dependent. In this work, the density-dependent coupling constants $g_\sigma(\rho)$ and $g_\omega(\rho)$ are extracted from the calculation of the relativistic Dirac-Brueckner-Hartree-Fock approach. By requiring the reproduction of the ratios $\Sigma_S(\rho)/\Sigma_S(\rho_0)$ and $\Sigma_0(\rho)/\Sigma_0(\rho_0)$ of the relativistic Dirac-Brueckner-Hartree-Fock calculations performed by Brockmann and Machleidt [28] at the same ρ/ρ_0, the $g_\sigma(\rho)$ and $g_\omega(\rho)$ can be parametrized as

$$g_\sigma^2(\rho)=\frac{g_\sigma^2(\rho_0)}{0.7941+0.2121(\rho/\rho_0)-0.0062(\rho/\rho_0)^2},$$
$$g_\omega^2(\rho)=\frac{g_\omega^2(\rho_0)}{0.6150+0.4347(\rho/\rho_0)-0.0497(\rho/\rho_0)^2}, \quad (8)$$

where $g_\sigma^2(\rho_0)$ and $g_\omega^2(\rho_0)$ are the effective coupling constants of the σ meson and the ω meson in normal nuclear matter, respectively. We observe that the effective coupling constants decrease with increasing density in Eq. (8).

It is well known that the self-energy of a nucleon in nuclear matter is identified with the effective interaction of the nucleon with the nuclear matter, i.e., the microscopic optical potential of a nucleon. The nucleon self-energy is a function of the four-momentum of the nucleon and the temperature and density of the nuclear matter. The space dependence of the temperature-dependent microscopic optical potential is directly connected with the density of the nuclear matter. Thus the Dirac equation of a nucleon in the nuclear medium reads

$$[(1+\Sigma_V)\vec{\alpha}\cdot\vec{k}+\gamma^0(m+\Sigma_S)+\Sigma_0]\psi(\vec{r})=E\psi(\vec{r}), \quad (9)$$

where the self-energy of a nucleon is complex and energy, temperature, and density dependent. It is convenient to rewrite Eq. (9) in terms of scalar and vector potentials only:

$$[\vec{\alpha}\cdot\vec{k}+\gamma_0(M+U_S)+U_0]\psi=E\psi, \quad (10)$$

where

$$U_S(k_\mu,\beta,\rho)=\frac{\Sigma_S(k_\mu,\beta,\rho)-m\Sigma_V(k_\mu,\beta,\rho)}{1+\Sigma_V(k_\mu,\beta,\rho)}$$
$$=V_S(k_\mu,\beta,\rho)+iW_S(k_\mu,\beta,\rho),$$
$$U_0(k_\mu,\beta,\rho)=\frac{\Sigma_0(k_\mu,\beta,\rho)-E\Sigma_V(k_\mu,\beta,\rho)}{1+\Sigma_V(k_\mu,\beta,\rho)}$$
$$=V_0(k_\mu,\beta,\rho)+iW_0(k_\mu,\beta,\rho). \quad (11)$$

To obtain the scattering amplitude, a Schrödinger-type equation is obtained by proper transformation. The large component of a nucleon wave function with the incident energy $\varepsilon=E-m$ obeys the equation

$$\left[\frac{k^2}{2E}+U_{\rm eff}+U_{\rm so}\vec{\sigma}\cdot\vec{L}\right]\phi=\frac{E^2-m^2}{2E}\phi, \quad (12)$$

where the temperature and density dependence of Schrödinger equivalent potentials $U_{\rm eff}$ and $U_{\rm so}$ are the central and spin-orbit ones, respectively, and

$$U_{\rm eff}=U_0+\frac{1}{2E}[U_S(U_S+2M)-U_0^2]. \quad (13)$$

The momentum of nucleon propagating through uniform nuclear matter is described by the dispersion relation

$$\varepsilon=\frac{k^2}{2m}+U_{\rm eff}(k,\varepsilon,\beta,\rho). \quad (14)$$

Since the Schrödinger equivalent potential $U_{\rm eff}$ is complex, the nucleon momentum k is also complex and can be expressed as

$$k=k_R+ik_I. \quad (15)$$

The nucleon mean free path λ is defined [3] by

$$\lambda=\frac{1}{2k_I}. \quad (16)$$

The explicit expression of the mean free path is obtained as

$$\lambda=-\frac{\sqrt{2m(\varepsilon-{\rm Re}U_{\rm eff})}}{2m^*{\rm Im}U_{\rm eff}}=-\frac{\{4mE[2E(\varepsilon-V_0)-V_S(2m+V_S)+V_0^2+W_S^2-W_0^2]\}^{1/2}}{2m^*[W_0+W_S(2m+V_S)+V_SW_S-2V_0W_0]}, \quad (17)$$

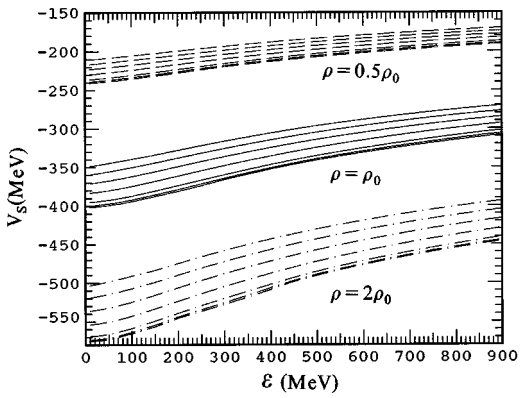

FIG. 2. The real part (V_S) of the nucleon scalar self-energy as a function of energy (ε), temperature (T), and density [$\rho(\mathrm{fm}^{-3})$]. The curves correspond to temperatures 50, 40, 30, 20, 10, 5, and 1 MeV from top to bottom, respectively.

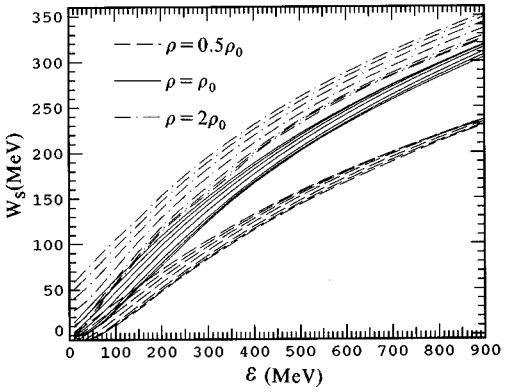

FIG. 4. The imaginary part (W_S) of the nucleon scalar self-energy as a function of energy (ε), temperature (T), and density [$\rho(\mathrm{fm}^{-3})$]. The curves correspond to temperatures is 50, 40, 30, 20, 10, 5, and 1 MeV from top to bottom, respectively.

where V_S, W_S, V_0, and W_0 are the real and imaginary part of the nucleon scalar and vector self-energy, respectively.

III. RESULTS AND DISCUSSIONS

In our calculations the effective coupling strengths are $g_\sigma^2(\rho_0)/4\pi=6.6137$, $g_\omega^2(\rho_0)/4\pi=8.59835$ for normal nuclear matter [19]. More results and discussions concerning the effective coupling strength in normal nuclear matter can be found in Refs. [19,22,25]. The numerical results of the dependence of the chemical potential μ on nuclear density ρ and temperature T are used as input for the calculation. $\rho_0=0.193\ \mathrm{fm}^{-3}$ is the density of normal nuclear matter. Both the real and imaginary parts of the nucleon self-energy as well as the corresponding mean free path have been calculated for different nuclear matter densities at various temperatures and incident energies.

Figures 2 and 3 show the real part of the nucleon scalar and vector self-energy, respectively. On the horizontal axis of Figs. 2–8, the nucleon energies $\varepsilon=E-m$ are given. We consider three cases with density $\rho=\frac{1}{2}\rho_0$ (dashed curves), $\rho=\rho_0$ (solid curves) and $\rho=2\rho_0$ (doted-dashed curves). The nuclear temperatures are 1, 5, 10, 20, 30, 40, and 50 MeV, respectively. We observe that the real part of the nucleon scalar self-energy increases with increasing incident nucleon energy and nuclear temperatures. The real part of the scalar nucleon self-energy depends strongly on the nuclear matter density and decreases with increasing nuclear density. The real part of the nucleon vector self-energy deceases with increasing incident nucleon energy, nuclear temperature, and density, and they do not change dramatically with increasing temperature at high energy and low density. The changes of the real part of the nucleon scalar and vector self-energy with the nuclear temperature and the incident nucleon energy becomes larger as the nuclear matter density increases and the energy dependence of the vector self-energy is stronger than that of the scalar self-energy with increasing nuclear density. The imaginary part of the nucleon scalar and vector self-energy as a function of the incident nucleon energy, nuclear temperature, and density are shown in Figs. 4 and 5, respectively. The imaginary part of the scalar and vector self-energy depend strongly on the incident nucleon energy and the nuclear density, those of the scalar self-energy increase with increasing incident nucleon energy, nuclear density and temperature, while those of the vector self-energy decrease as the incident nucleon energy, nuclear density, and tempera-

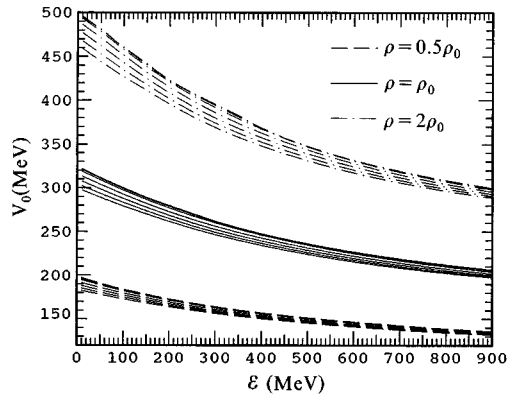

FIG. 3. The real part (V_0) of the nucleon vector self-energy as a function of energy(ε), temperature (T) and density [$\rho(\mathrm{fm}^{-3})$]. The curves correspond to temperatures 1, 5, 10, 20, 30, 40, and 50 MeV from top to bottom, respectively.

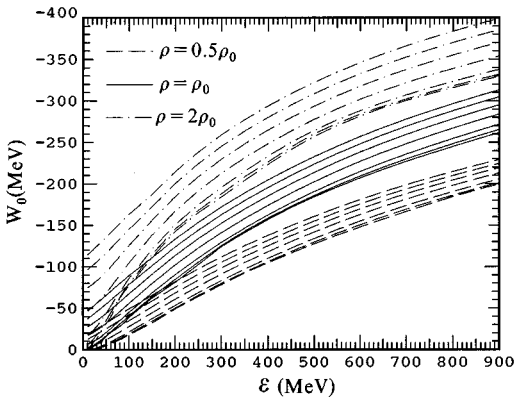

FIG. 5. The imaginary part (W_0) of the nucleon vector self-energy as a function of energy (ε), temperature (T) and density [$\rho(\mathrm{fm}^{-3})$]. The curves correspond to temperatures 50, 40, 30, 20, 10, 5, and 1 MeV from top to bottom, respectively.

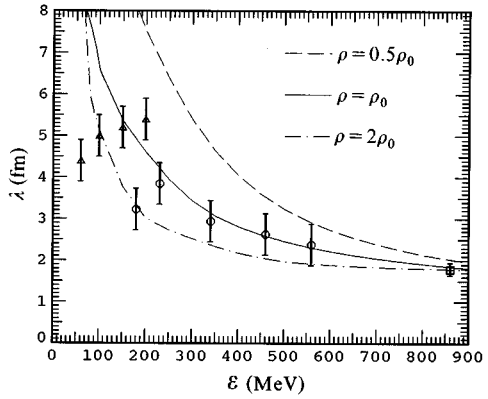

FIG. 6. The nucleon mean free path (λ) as a function of energy (ε) and density [$\rho(\mathrm{fm}^{-3})$] at zero temperature (T). The triangles with error bars are from Ref. [34], the dots with error bars are from Ref. [21], and the squares with error bars are from Ref. [20].

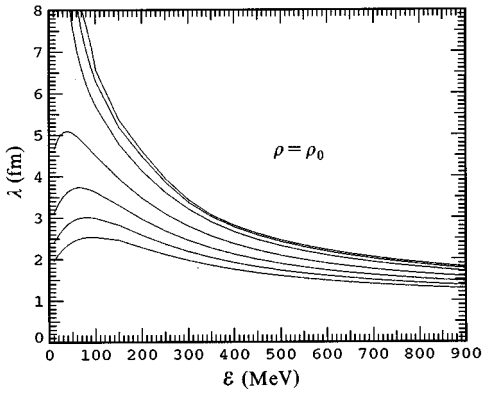

FIG. 7. The nucleon mean free path (λ) as a function of energy (ε), and temperature (T) at the normal matter density (ρ_0). The curves correspond to temperatures 1, 5, 10, 20, 30, 40, and 50 MeV from top to bottom, respectively.

ture increase. The change of the imaginary part of the nucleon scalar and vector self-energy with temperature becomes larger with increasing nuclear density. The imaginary part of the nucleon vector self-energy changes more dramatically than that of the scalar self-energy with increasing temperature and density.

The comparison of the calculated values of the nucleon mean free path with experimental data [20,21] is shown in Fig. 6. The dot and square with error bars are experimental data [20,21] and the triangle with error bars indicates the estimation of the nucleon mean free path based on total reaction cross sections [34]. We observe that our calculated results are in reasonable agreement with experimental data and empirical data in the incident nucleon energy $\varepsilon \geqslant 100$ MeV for normal nuclear matter. Compared to the recent empirical data based on Dirac phenomenology in an energy-dependent analysis [14,15] and the relativistic calculated results in Refs. [11,16], our calculated results are slightly larger while in the energy region. Comparing the present calculated results on the nucleon mean free path based on the relativistic model with those based on the nonrelativistic model in Refs. [8,9], we have found that the agreement in tendency between them is quite good for energy $\varepsilon < 60$ MeV, however, the values of the present calculation are larger than those in Refs. [8,9]. The reason for this difference lies in the fact that the effective mass of the nucleon in the relativistic model is smaller than that in the nonrelativistic model, and the imaginary part of the Schrödinger equivalent potential of the relativistic microscopic optical potential which depends on the effective mass of the nucleon in the relativistic model is shallower than that of the optical potential in the nonrelativistic model [8,9]. It should be mentioned that the results obtained in Refs. [8,9] are valid to incident nucleon energy $\varepsilon \leqslant 60$ MeV due to the limitation of the Skyrme interaction [35] implemented there as discussed in those papers, while for the incident nucleon energy $\varepsilon > 60$ MeV, the present results based on Walecka's model are more reasonable than those in Refs. [8,9]. Also of interest is the density dependence of the nucleon mean free path. In Fig. 6 we also show the density dependence of the nucleon mean free path as a function of the incident nucleon energy. The nucleon mean free path decreases with increasing nuclear density, especially at low density and low energy. The change of the nucleon mean free path with the incident nucleon energy is smaller at high density for energy $\varepsilon \geqslant 300$ MeV. The temperature and density dependence of the nucleon mean free path as a function of the incident nucleon energy are shown in Figs. 7 and 8. The nucleon mean free path comes from the contribution of the correlation diagram for low energy (or momentum $k < k_F$). We observe that the nucleon mean free path decreases with increasing nuclear temperature, especially at low energy. The nucleon mean free path depends weakly on the incident nucleon energy for the high temperature and density considered here. The change of the nucleon mean free path with nuclear temperature is more dramatic than those with nuclear matter density, especially for high energy ($\varepsilon \geqslant 600$ MeV).

IV. SUMMARY AND CONCLUSION

We have studied the nuclear temperature and density dependence of the nucleon self-energy and mean free path based on Walecka's model, the thermofield dynamics, and the relativistic Dirac-Brueckner-Hartree-Fock results in this paper, and the whole contributions of the fourth Feynman

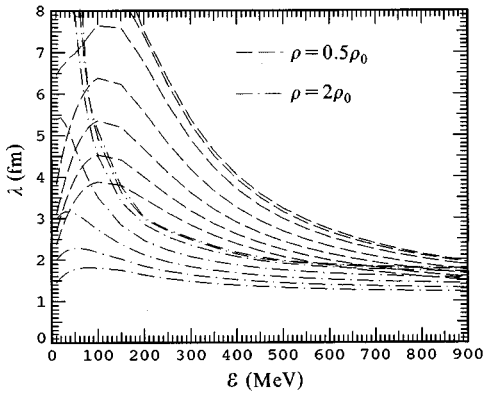

FIG. 8. The nucleon mean free path (λ) as a function of energy (ε), temperature (T), and density [$\rho(\mathrm{fm}^{-3})$]. The curves correspond to temperatures 1, 5, 10, 20, 30, 40, and 50 MeV from top to bottom, respectively.

diagram have been taken into account. The density-dependent coupling constants of this effective Lagrangian are determined from the relativistic Dirac-Brueckner-Hartree-Fock results for nuclear matter.

The nucleon self-energy depends strongly on the nuclear matter density; especially the real part of them. The real part of the nucleon scalar self-energy becomes deeper and that of the nucleon vector self-energy becomes shallower with increasing nuclear matter density, while the imaginary part of the nucleon scalar self-energy becomes shallower and that of the nucleon vector self-energy becomes deeper with increasing nuclear matter density. The nucleon scalar self-energy becomes shallower and the nucleon vector self-energy becomes deeper with increasing temperature. The change of the nucleon self-energy with temperature becomes larger as the nuclear matter density increases.

The temperature and density dependence of the nucleon mean free path are calculated from the Schrödinger equivalent potential of the relativistic microscopic optical potential. Our calculated results for the nucleon mean free path in normal nuclear matter are in good agreement with the experimental data and the empirical data at zero temperature. The nucleon mean free path decreases with increasing nuclear temperature and density, and the change of them with temperature is more dramatic than that with density, especially for high energy.

ACKNOWLEDGMENT

This work was supported by the National Natural Science Foundation of China.

[1] J. P. Schiffer, Nucl. Phys. **A335**, 348 (1980).
[2] M. T. Collins and J. J. Griffin, Nucl. Phys. **A348**, 63 (1980).
[3] J. W. Negele and K. Yazaki, Phys. Rev. Lett. **47**, 71 (1981).
[4] H. O. Meyer and P. Schwandt, Phys. Lett. **107B**, 353 (1981).
[5] S. Fantoni, B. L. Friman, and V. R. Pandharipande, Phys. Lett. **161B**, 89 (1983).
[6] Bikash Sinha, Phys. Rev. Lett. **50**, 91 (1983).
[7] A. H. Blin, R. W. Hasse, B. Hiller, and P. Schuck, Phys. Lett. **161B**, 211 (1985).
[8] L. X. Ge, Y. Z. Zhuo, and W. Norenbery, Nucl. Phys. **A459**, 77 (1986).
[9] Yizhong Zhuo, Yinlu Han, and Xizheng Wu, Prog. Theor. Phys. **76**, 110 (1988).
[10] Han Yinlu, Mao Guangjun, Li Zhuxia, and Zhuo Yizhong, Phys. Rev. C **50**, 961 (1994).
[11] T. Chen, Phys. Rev. C **38**, 1516 (1988).
[12] R. A. Rego, Phys. Rev. C **44**, 1944 (1991).
[13] Han Yin-lu, Shen Qing-biao, and Zhuo Yi-zhong, Phys. Rev. C **46**, 2396 (1992).
[14] E. D. Cooper, S. Hama, B. C. Clark, and R. L. Mercer, Phys. Rev. C **47**, 297 (1993).
[15] B. C. Clark, E. D. Cooper, S. Hama, R. W. Finlay, and T. Adami, Phys. Lett. B **229**, 189 (1993).
[16] G. Q. Li, R. Machleidt, and Yizhong Zhuo, Phys. Rev. C **48**, 1062 (1993).
[17] Mao Guangjun, Li Zhuxia, Zhuo Yizhong, Han Yinlu, Yu Ziqiang, and M. Sano, Z. Phys. A **347**, 173 (1994).
[18] Yin-lu Han, Qing-biao Shen, Yi-zhong Zhuo, and Tian-ming Geng, Nucl. Phys. **A569**, 732 (1994).
[19] B. D. Serot and J. D. Walecka, Adv. Nucl. Phys. **16**, 1 (1985).
[20] F. F. Chen, C. P. Leavitt, and A. M. Shapiro, Phys. Rev. **99**, 857 (1955).
[21] P. U. Renberg, D. F. Measday, M. Pepin, P. Schwaller, B. Favier, and C. Richard-Serre, Nucl. Phys. **A183**, 81 (1972).
[22] C. J. Horowitz and B. D. Serot, Nucl. Phys. **A399**, 529 (1983).
[23] C. J. Horowitz, Nucl. Phys. **A412**, 228 (1984).
[24] J. D. Walecka, Ann. Phys. (N.Y.) **83**, 83 (1974).
[25] Ma Zhongyu, Zhu Ping, Gu Yingqi, and Zhuo Yizhong, Nucl. Phys. **A490**, 619 (1988).
[26] Qinbiao Shen, Dachung Feng, and Zhuo Yizhong, Phys. Rev. C **43**, 2773 (1991).
[27] R. Machleidt, Adv. Nucl. Phys. **19**, 189 (1989).
[28] R. Brockmann and R. Machleidt, Phys. Rev. C **42**, 1965 (1990).
[29] L. Leplae, H. Umezawa, and F. Mancini, Phys. Rep. **10**, 151 (1974).
[30] Y. Takahashi and H. Umezawa, Collect. Phenom. **2**, 55 (1975).
[31] K. Saito, T. Maruyama, and K. Soutome, Phys. Rev. C **40**, 407 (1989).
[32] K. Soutome, T. Maruyama, and K. Saito, Nucl. Phys. **A507**, 731 (1990).
[33] R. Brockmann and H. Toki, Phys. Rev. Lett. **68**, 3408 (1992).
[34] A. Nadasen *et al.*, Phys. Rev. C **23**, 1023 (1981).
[35] T. H. R. Skyrme, Nucl. Phys. **9**, 615 (1959).